PHYSICAL REVIEW D **94,** 076009 (2016)

QCD phase transitions via a refined truncation of Dyson-Schwinger equations

Fei Gao[1,2] and Yu-xin Liu[1,2,3,*]

[1]*Department of Physics and State Key Laboratory of Nuclear Physics and Technology, Peking University, Beijing 100871, China*

[2]*Collaborative Innovation Center of Quantum Matter, Beijing 100871, China*

[3]*Center for High Energy Physics, Peking University, Beijing 100871, China*

(Received 7 July 2016; published 31 October 2016)

We investigate both the chiral and deconfinement phase transitions of QCD matter in a refined scheme of Dyson-Schwinger equations, which have been shown to be successful in giving the meson mass spectrum and matching the interaction with the results from *ab initio* computation. We verify the equivalence of the chiral susceptibility criterion with different definitions for the susceptibility and confirm that the chiral susceptibility criterion is efficient to fix not only the chiral phase boundary but also the critical end point (CEP), especially when one could not have the effective thermodynamical potential. We propose a generalized Schwinger function criterion for the confinement. We give the phase diagram of both phase transitions and show that in the refined scheme the position of the CEP shifts to lower chemical potential and higher temperature. Based on our calculation and previous results of the chemical freeze-out conditions, we propose that the CEP is located in the states of the matter generated by the Au–Au collisions with $\sqrt{s_{NN}} = 9$–15 GeV.

DOI: 10.1103/PhysRevD.94.076009

I. INTRODUCTION

The phase diagram of strong interaction matter in the plane of temperature T and chemical potential μ has been investigated for a long time (for recent reviews, see, e.g., Refs. [1–3]). The strong interaction is described by QCD which includes two important features, dynamical chiral symmetry breaking and confinement, and thus the phase transitions are denoted as the QCD phase transitions and classified into two kinds: the dynamical chiral symmetry breaking (DCSB)-dynamical chiral symmetry (DCS) phase transition and the confinement-deconfinement phase transition. To determine the order and the phase boundary of the chiral phase transition, thousands of works have taken the chiral susceptibility criterion to carry out the investigations (see, e.g., Refs. [4–52]). Since the system usually involves multiple variables, in turn, there are different definitions for the chiral susceptibility. The equivalence between the differently defined susceptibilities in signalling the phase transition has not yet been examined thoroughly. Even the equivalence of the susceptibility criterion to the thermodynamical potential criterion has not yet been clarified, either, except in some simple models (see, e.g., Ref. [52]). For the confinement-deconfinement phase transition, since the confinement is defined as the color degrees of freedom being confined within hadrons and not observable as isolated states, it can naturally be associated with the positivity violation of the spectral density function. The positivity of the spectral density function is then sufficient to label the deconfinement [53,54]. Because of the difficulties in calculating the spectral function, one usually evaluates the Schwinger function, which is defined as the Fourier transformation of the propagator (at finite temperature and finite chemical potential) [55–62]. Nevertheless, the Schwinger function criterion fails in some cases [63] because the Schwinger function is the integral of the spectral density. It is then necessary to extend the Schwinger function so that the criterion is equivalent to that of the spectral density function, and the numerical calculation is easy to carry out.

It has been well known that the QCD phase transitions happen at the energy scale 10^2 MeV, and one must take nonperturbative QCD approaches to accomplish the investigations. Therefore, lattice QCD simulations have been widely implemented (see, e.g., Refs. [3,5,7–26]). However, the "sign problem" [3] prevents it from making rapid progress in the large chemical potential region. The Dyson-Schwinger (DS) equation method [53,54,64–68] and the functional renormalization group approach [69], which include both the DCSB and the confinement inherently [70,71], have thus played the role. Not only the general features of the phase transitions but also some detailed aspects, such as the critical end point (CEP), the property of the state in the temperature region above but near the pseudocritical one, the baryon number fluctuations and some transport properties, have then been proposed (see, e.g., Refs. [27–34,55–62,71–82]). The DS equation approach of QCD is a method of continuum quantum field theory. It is convenient to stretch the calculations on the whole μ–T plane without further approximation. This

*yxliu@pku.edu.cn.

advantage makes it better to obtain the information of the phase structure on the μ–T plane than the lattice QCD simulations in the case of large chemical potential at the present stage. However, many of the previous work via the DS equation approach were based on the bare approximation for the quark-gluon interaction vertex. On the hadron property side, which is usually taken as the calibration to fix the parameter(s) in the DS equation approach, it has been shown that the bare vertex truncation is accurate for light-flavor ground-state vector- and isospin-nonzero-pseudoscalar mesons [65,67,68,83] because corrections in these channels largely cancel each other, owing to the parameter-free preservation of the Ward-Green-Takahashi (WGT) identities [84–86]. This truncation is also reasonable for heavy-flavor quarkonia [87]. Since the corrections do not cancel in other channels [88–91], studies based on such a truncation have not usually provided excellent results for scalar, axial-vector, and exotic state mesons [92–98] and have exhibited gross sensitivity to model parameters for excited states [97–100] and tensor mesons [101]. Meanwhile, some investigations have shown that extending the bare vertex approximation to systematic truncation may not only improve the results for mesons (see, e.g., Refs. [91,102–104]) but also be promising for the phase transitions in QCD (see, e.g., Refs. [27–29,32,33,77,105]) and QED (see, e.g., Refs. [106–108]).

A recently developed truncation scheme with a concise expression for the quark-gluon interaction vertex [102,109] has been found to have bridged the bottom-up scheme with the *ab initio* computation in continuum QCD [110]. The scheme preserves the WGT identities [105,111,112] and introduces the DCSB effect into the interaction kernel [105,109]. It has successfully given realistic hadron properties for not only the ground states of axial-vector mesons but also some exited-state mesons [102]. Considering the success in describing the hadron properties of the new scheme and the coincidence with the *ab initio* computation, it is imperative to implement the refined scheme to reanalyze the phase transitions in the T–μ plane and examine the discrepancy of the results induced by the difference of the truncation schemes.

We then take the refined truncation scheme to investigate the QCD phase transitions in this paper. After analyzing the chiral susceptibility criterion for the chiral phase transition and generalizing the Schwinger function criterion for the confinement phase transition, we obtain the phase diagrams of the transitions. We show that the two kinds of phase transitions coincide with each other and the results of the chiral susceptibility criteria with different definitions for the susceptibility deviate only in the crossover region slightly due to the nature of the crossover. We verify that the phase transition temperature at zero chemical potential is (at least) 150 MeV, which is consistent with the lattice QCD results, and propose that the CEP of the chiral phase transition is located at $(\mu_B, T) = (262, 126)$ MeV. It indicates that the refined truncation decreases the chemical potential of the CEP. Such a location of the CEP is in the range of the states able to be generated with the $\sqrt{s} \cong 9$–15 GeV Au-Au collision with the parametrization of the energy dependence of μ [78,113–115] and, in turn, may be observed in the beam energy scan experiments at the Relativistic Heavy Ion Collider (RHIC) [116,117].

The remainder of this paper is organized as follows. In Sec. II, we reiterate briefly the DS equation approach and its refined truncation scheme. In Sec. III, we analyze the criteria of the chiral phase transition, show their equivalence, and emphasize the efficiency of the chiral susceptibility criterion in fixing the CEP. In Sec. IV, we extend the Schwinger function criterion and show the equivalence between the generalized Schwinger function and the spectral density function. In Sec. V, we give our results of the phase diagrams and discuss the properties. Finally, we summarize in Sec. IV.

II. QUARK GAP EQUATION

In the DS equation approach of QCD, the quark propagator S at finite temperature T and finite quark chemical potential μ_q can be determined with the gap equation

$$S(\vec{p},\tilde{\omega}_n)^{-1} = i\vec{\gamma}\cdot\vec{p} + i\gamma_4\tilde{\omega}_n + m_0 + \Sigma(\vec{p},\tilde{\omega}_n), \quad (1)$$

$$\Sigma(\vec{p},\tilde{\omega}_n) = T\sum_{l=-\infty}^{\infty}\int\frac{d^3q}{(2\pi)^3}g^2D_{\mu\nu}(\vec{p}-\vec{q},\Omega_{nl};T,\mu_q) \times\frac{\lambda^a}{2}\gamma_\mu S(\vec{q},\tilde{\omega}_l)\frac{\lambda^a}{2}\Gamma_\nu(\vec{q},\tilde{\omega}_l,\vec{p},\tilde{\omega}_n), \quad (2)$$

where m_0 is the current quark mass, $\tilde{\omega}_n = \omega_n + i\mu_q$ with $\omega_n = (2n+1)\pi T$ being the quark Matsubara frequency and μ_q the quark chemical potential; $\Omega_{nl} = \omega_n - \omega_l$; $g^2D_{\mu\nu}(\vec{p}-\vec{q},\Omega_{nl};T,\mu_q)$ is the interaction with $D_{\mu\nu}$ the dressed-gluon propagator; and Γ_ν is the dressed-quark-gluon vertex. The gap equation's solution can be decomposed as

$$S(\vec{p},\tilde{\omega}_n)^{-1} = i\vec{\gamma}\cdot\vec{p}A(\vec{p}^2,\tilde{\omega}_n^2) + i\gamma_4\tilde{\omega}_nC(\vec{p}^2,\tilde{\omega}_n^2) + B(\vec{p}^2,\tilde{\omega}_n^2). \quad (3)$$

To get the functions $A(\vec{p}^2,\tilde{\omega}_n^2)$, $B(\vec{p}^2,\tilde{\omega}_n^2)$, and $C(\vec{p}^2,\tilde{\omega}_n^2)$ by solving the gap equation, one must take appropriate truncation(s), in other words, have the expressions of Γ_μ and $g^2D_{\mu\nu}(\vec{p}-\vec{q},\Omega_{nl};T,\mu_q)$. In our calculations, we implement the refined truncation to the quark-gluon interaction vertex [109], which would be called the anomalous chromomagnetic moments (ACM) kernel or Chang-Liu-Roberts (CLR) kernel, which reads

$$\Gamma_\mu = \Gamma_\mu^{\mathrm{BC}} + \Gamma_\mu^{\mathrm{ACM}}, \quad (4)$$

$$\Gamma_\mu^{\rm ACM}=\Gamma_\mu^{\rm ACM_4}+\Gamma_\mu^{\rm ACM_5}. \tag{5}$$

The $\Gamma_\mu^{\rm BC}$, which is just the Ball-Chiu (BC) vertex [118], can be proven to be the unique longitudinal part of the vertex constrained by combining the longitudinal and the transverse WGT identities [111,112]. The generalized form of the BC vertex at finite temperature [28,74,119] reads

$$\begin{aligned}&\Gamma_\mu^{\rm BC}(\vec{q},\tilde{\omega}_l,\vec{p},\tilde{\omega}_n)\\&=\gamma_\mu^T\Sigma_A+\gamma_\mu^L\Sigma_C+(p_n+q_l)_\mu\Big[\frac{1}{2}\gamma_\alpha^T(p_n+q_l)_\alpha\Delta_A\\&\quad+\frac{1}{2}\gamma_\alpha^L(p_n+q_l)_\alpha\Delta_C-i\Delta_B\Big],\end{aligned} \tag{6}$$

with

$$\begin{aligned}&p_n=(\vec{p},\tilde{\omega}_n),\qquad q_l=(\vec{q},\tilde{\omega}_l),\\&\Sigma_F(\vec{q}^2,\tilde{\omega}_l^2,\vec{p}^2,\tilde{\omega}_n^2)=\frac{1}{2}[F(\vec{q}^2,\tilde{\omega}_l^2)+F(\vec{p}^2,\tilde{\omega}_n^2)],\\&\Delta_F(\vec{q}^2,\tilde{\omega}_l^2,\vec{p}^2,\tilde{\omega}_n^2)=\frac{F(\vec{q}^2,\tilde{\omega}_l^2)-F(\vec{p}^2,\tilde{\omega}_n^2)}{q_l^2-p_n^2},\end{aligned} \tag{7}$$

where $F=A$, B, C, and $\gamma_\mu^T=\gamma_\mu-\gamma_\mu^L$, $\gamma_\mu^L=u_\mu\gamma_\alpha u_\alpha$ with $u=(0,0,0,1)$.

The $\Gamma_\mu^{\rm ACM}$ is the transverse part in the vertex that characterizes the DCSB effect in the quark-gluon vertex through the ACM [109], which reads

$$\Gamma_\mu^{\rm ACM_4}=[T_{\mu\nu}l_\nu\gamma\cdot k+iT_{\mu\nu}\gamma_\nu\sigma_{\rho\sigma}l_\rho k_\sigma]\tau_4(p_n,q_l), \tag{8}$$

$$\Gamma_\mu^{\rm ACM_5}=\sigma_{\mu\nu}k_\nu\tau_5(p_n,q_l), \tag{9}$$

$$\tau_4=\frac{2\tau_5(p_n,q_l)[2(M(p_n^2)+M(q_l^2))]}{p_n^2+M(p_n^2)^2+q_l^2+M(q_l^2)^2}, \tag{10}$$

$$\tau_5=\eta\Delta_B, \tag{11}$$

where $\sigma_{\mu\nu}=(i/2)[\gamma_\mu,\gamma_\nu]$, $T_{\mu\nu}=\delta_{\mu\nu}-k_\mu k_\nu/k^2$, $k_\mu=(p_n-q_l)_\mu$, $l_\mu=\frac{(p_n+q_l)_\mu}{2}$, and $M(x)=B(x)/A(x)$, with p_n (p_l) and Δ_B defined in Eq. (7), and η is a parameter.

It has been mentioned that this truncation scheme satisfies both the longitudinal and transverse WGT identities [111,112] and makes the interaction match with the results obtained from *ab initio* computation [110]. Besides, the above expressions manifest that the refined quark-gluon interaction vertex is quite concise and easy to generalize to finite temperature and finite chemical potential.

The interaction together with the dressed-gluon propagator generally has the form

$$g^2D_{\mu\nu}(\vec{k},\Omega_{nl})=P_{\mu\nu}^TD_T(\vec{k}^2,\Omega_{nl}^2)+P_{\mu\nu}^LD_L(\vec{k}^2,\Omega_{nl}^2), \tag{12}$$

where $P_{\mu\nu}^{T,L}$ are, respectively, the transverse and longitudinal projection operators,

$$\begin{aligned}P_{\mu\nu}^T&=(1-\delta_{\mu4})(1-\delta_{\nu4})\Big(\delta_{\mu\nu}-\frac{p_\mu p_\nu}{p^2}\Big),\\P_{\mu\nu}^L&=\Big(\delta_{\mu\nu}-\frac{p_\mu p_\nu}{p^2}\Big)-P_{\mu\nu}^T,\end{aligned} \tag{13}$$

with $p=(\vec{p},\tilde{\omega}_n)$, the same as that in Eq. (7), and

$$\begin{aligned}D_L\Big(\vec{k}^2,\Omega_{nl}^2\Big)&=\mathcal{D}\Big(k_\Omega^2,m_g^2\Big),\\D_T\Big(\vec{k}^2,\Omega_{nl}^2\Big)&=\mathcal{D}\Big(k_\Omega^2,0\Big),\end{aligned} \tag{14}$$

where m_g is the thermal mass of the gluon and can be taken as $m_g^2=16/5(T^2+6\mu_q^2/(5\pi^2))$ according to perturbative QCD calculations [120,121].

The D_L should generally be different from the D_T at finite temperature and finite chemical potential as indicated in lattice QCD simulations (e.g., Refs. [122–124]) and coupled DS equations calculations (e.g., Refs. [29,32,33,77]). However, if we study the phase structure of the quark, then as a mediate input, $D_L=D_T$ is a tolerable approximation as shown in previous investigations (see, e.g., Refs. [28,30,31] and others). We take thus the approximation $D_T=D_L=\mathcal{D}(k_\Omega^2,0)$ to study the phase diagram with the effect of the refined quark-gluon vertex at the present stage. The modern DS equation and lattice QCD studies indicate that the gluon propagator is a bounded, regular function of spacelike momenta, which achieves its maximum value on the domain at $k^2=0$ [125–135]. We then employ an interaction which expresses these features [97,102,110] as

$$\begin{aligned}\mathcal{D}(k_\Omega^2,0)&=8\pi^2\mathcal{D}\frac{1}{\omega^4}e^{-s_\Omega/\omega^2}\\&\quad+\frac{8\pi^2\gamma_m}{\ln[\tau+(1+s_\Omega/\Lambda_{\rm QCD}^2)^2]}\mathcal{F}(s_\Omega),\end{aligned} \tag{15}$$

with $\mathcal{F}(s_\Omega)=(1-\exp(-s_\Omega/4m_t^2))/s_\Omega$, $\tau=e^2-1$, $m_t=0.5$ GeV, $\gamma_m=12/(33-2N_F)$ with N_F the flavor number, $\Lambda_{\rm QCD}=0.234$ GeV, $s_\Omega=\Omega^2+\vec{k}^2$, and $\mathcal{D}$ and ω parameters.

To carry out the renormalization in the ultraviolet region easily in practical calculation, we multiply an additional damping factor $[1-\exp(-s_\Omega)]/s_\Omega$ on the ultraviolet part of the dressed-gluon propagator, just as the Refs. [102,110] have practically done.

III. CHIRAL PHASE TRANSITION

A. Criteria for chiral phase transition

To investigate the chiral phase transition, the chiral susceptibilities have commonly been taken as the criteria.

The (generalized) chiral susceptibility is defined as the derivative of the chiral order parameter with respect to the control parameters, such as the current quark mass m_0, temperature T, and chemical potential μ. The susceptibility can be connected with the thermodynamical potential. To this end, we consider the Cornwall-Jackiw-Tomboulis effective thermodynamical potential for quarks, which reads [136]

$$\Gamma(S) = -\mathrm{Tr}[\ln(S_0^{-1}S) - S_0^{-1}S + 1] + \Gamma_2(S), \quad (16)$$

where S_0 stands for the bare quark propagator and Γ_2 represents the two-particle-irreducible (2PI) and higher order contributions. Calculating the variation with respect to the quark propagator, we have

$$\frac{\partial\Gamma}{\partial S} = -S^{-1} + S_0^{-1} + \frac{\partial\Gamma_2(S)}{\partial S}, \quad (17)$$

$$\frac{\partial^2\Gamma}{\partial S^2} = S^{-2} + \frac{\partial^2\Gamma_2(S)}{\partial S^2}. \quad (18)$$

The quark propagator's DS equation could be derived through the extreme condition of Eq. (17). Meanwhile, if calculating the derivative of the extreme condition with respect to the current quark mass for quark propagator's DS equation, we obtain

$$-S^{-2}\frac{\partial S}{\partial m_0} = 1 + \frac{\partial^2\Gamma_2(S)}{\partial S^2}\frac{\partial S}{\partial m_0}. \quad (19)$$

The function S represents the dynamical symmetry breaking and can be considered as an order parameter. The $\frac{\partial S}{\partial m_0}$ can then be regarded as a generalized chiral susceptibility, too. Comparing Eqs. (17) and (19), we can find straightforwardly the relation between the generalized chiral susceptibility and the thermodynamical potential,

$$\frac{\partial S}{\partial m_0} = -\frac{1}{\partial^2\Gamma/\partial S^2}. \quad (20)$$

Similar relations between $\frac{\partial S}{\partial T}$, $\frac{\partial S}{\partial \mu}$ and thermodynamical potential can also be easily derived as above.

It is well known that the sign changing of the second-order derivative of the thermodynamical potential at the state satisfying the extreme condition is conventionally regarded as the signature of a phase transition. When we consider the case in the nonperturbative point of view completely, we could not have the thermodynamical potential explicitly. The conventional thermodynamical criterion fails, unfortunately. We should then develop new criteria. From the above relations, one can notice that the (generalized) chiral susceptibility is the reciprocal of the second-order derivative of the thermodynamical potential (a similar relation in the case of the Nambu–Jona-Lasinio (NJL) model has been given in Ref. [52], and a not-so-concise expression in DS equation of QCD has also been given in Refs. [137,138]). It means that the (generalized) chiral susceptibilities play the same role as the thermodynamical potential in identifying the chiral phase transition and can thus be taken as criteria for the transition.

It is also well known that, in the case of the chiral limit, the trace of the quark propagator is the chiral quark condensate $\langle\bar{q}q\rangle$. Extending such a definition to the case beyond chiral limit, we have

$$\begin{aligned}\langle\bar{q}q\rangle_{m_0} &= \mathrm{Tr}[S(p)_{m_0\neq 0}] \\ &= -Z_4 N_c N_f \int \frac{d^4p}{(2\pi)^4}\mathrm{tr}[S(p)_{m_0\neq 0}], \end{aligned} \quad (21)$$

where Z_4 is the renormalization constant, N_c is the number of colors, and N_f is the number of flavors. However, the direct trace of the quark propagator in case of nonvanishing current quark mass contains quadratic divergence. Some subtraction schemes must be taken when calculating the condensate. Noticing that the quark mass function could be written as [53]

$$\begin{aligned} M(-Q^2) &= \frac{B(-Q^2)}{A(-Q^2)} \\ &\overset{Q^2\to\infty}{\longrightarrow} \frac{c}{Q^2}\left[\ln\left(\frac{Q^2}{\Lambda_{\mathrm{QCD}}^2}\right)\right]^{\gamma_m - 1} \\ &\quad + m_0\left[\frac{\ln(\mu^2/\Lambda_{\mathrm{QCD}}^2)}{\ln(Q^2/\Lambda_{\mathrm{QCD}}^2)}\right]^{\gamma_m}, \end{aligned} \quad (22)$$

with $c = -\frac{4\pi^2\gamma_m}{3}\frac{\langle\bar{q}q\rangle}{[\ln(\mu^2/\Lambda_{\mathrm{QCD}}^2)]^{\gamma_m}}$ and μ as the renormalization scale, one can find that the quadratic divergence is linearly dependent on the current quark mass m_0. It is apparent that the quadratic divergence can be removed when the quark condensate is redefined along the lines of Ref. [139] as

$$\langle\bar{q}q\rangle = \langle\bar{q}q\rangle_{m_0} - m_0\frac{\partial\langle\bar{q}q\rangle_{m_0}}{\partial m_0}. \quad (23)$$

It is evident that the quark condensate is a direct measure of the dynamical quark mass generation. This condensate has then commonly been taken as the chiral order parameter. As the integral is extended to that at finite temperature and/or finite chemical potential, the responsibilities $\frac{\partial\langle\bar{q}q\rangle}{\partial T}$, $\frac{\partial\langle\bar{q}q\rangle}{\partial\mu}$, $\frac{\partial\langle\bar{q}q\rangle}{\partial m_0}$, and so on are also regarded as the chiral susceptibility and could naturally be taken as the signatures of the chiral phase transition, which are much more concrete than the ones expressed similar to Eq. (20).

To show more intuitively the equivalence of the chiral susceptibility criterion with the thermodynamical potential criterion, we recall Eqs. (16), (21), and (23). It is apparent that the thermodynamical potential can be rewritten as

$$\Gamma(S) = \Gamma(\langle\bar{q}q\rangle).$$

Along the line of the Landau phase transition theory, the above thermodynamical potential of the state around the phase transition can be expanded in terms of the powers of the condensate as

$$\Gamma(\langle\bar{q}q\rangle,\zeta) = \Gamma_0(\zeta) + \frac{1}{2}\alpha\langle\bar{q}q\rangle^2 + \frac{1}{4}\beta\langle\bar{q}q\rangle^4 + \frac{1}{6}\gamma\langle\bar{q}q\rangle^6, \tag{24}$$

where ζ denotes all the controlling variables such as temperature T, chemical potential μ, and so on, α, β, and γ are the interaction strength parameters depending on the intrinsic property of the system and controlling variables. We have then the other form of the generalized chiral susceptibility,

$$\chi = \frac{\partial\langle\bar{q}q\rangle}{\partial\zeta}. \tag{25}$$

After differentiating the stationary condition of the effective thermodynamical potential with respect to the controlling parameter, one can easily have

$$\begin{aligned}\chi &= \frac{-\langle\bar{q}q\rangle\left(\frac{\partial\alpha}{\partial\zeta}\right)_{\zeta=\zeta_c} - \langle\bar{q}q\rangle^3\left(\frac{\partial\beta}{\partial\zeta}\right)_{\zeta=\zeta_c} - \langle\bar{q}q\rangle^5\left(\frac{\partial\gamma}{\partial\zeta}\right)_{\zeta=\zeta_c}}{\alpha + 3\beta\langle\bar{q}q\rangle^2 + 5\gamma\langle\bar{q}q\rangle^4} \\ &= -\frac{\langle\bar{q}q\rangle\left(\frac{\partial\alpha}{\partial\zeta}\right)_{\zeta=\zeta_c} + \langle\bar{q}q\rangle^3\left(\frac{\partial\beta}{\partial\zeta}\right)_{\zeta=\zeta_c} + \langle\bar{q}q\rangle^5\left(\frac{\partial\gamma}{\partial\zeta}\right)_{\zeta=\zeta_c}}{\left(\frac{\partial^2\Gamma}{\partial\langle\bar{q}q\rangle^2}\right)_{\frac{\partial\Gamma}{\partial\langle\bar{q}q\rangle}=0}}.\end{aligned}$$

It is also known that, for the symmetry restoration phase transition, the derivatives $(\frac{\partial\alpha}{\partial\zeta})_{\zeta=\zeta_c} > 0$, $(\frac{\partial\beta}{\partial\zeta})_{\zeta=\zeta_c} > 0$, and $(\frac{\partial\gamma}{\partial\zeta})_{\zeta=\zeta_c} > 0$. Since $\langle\bar{q}q\rangle < 0$, such a susceptibility χ takes the same sign as the $(\frac{\partial^2\Gamma}{\partial\langle\bar{q}q\rangle^2})_{\frac{\partial\Gamma}{\partial\langle\bar{q}q\rangle}=0}$. One can then recognize that, if the chiral susceptibility is positive, the state is in a stable phase, and the negative susceptibility stands for an unstable phase. The divergence of χ [corresponding to $(\frac{\partial^2\Gamma}{\partial\langle\bar{q}q\rangle^2})_{\frac{\partial\Gamma}{\partial\langle\bar{q}q\rangle}=0} = 0$] identifies the phase transition apparently. Therefore, the susceptibilities play the same role as the thermodynamical potential in identifying the phase transition, and $\frac{\partial\langle\bar{q}q\rangle}{\partial T}$, $\frac{\partial\langle\bar{q}q\rangle}{\partial\mu}$, and $\frac{\partial\langle\bar{q}q\rangle}{\partial m_0}$ have been commonly taken as the signatures for the chiral phase transition, no matter whether the thermodynamical potential is valid or not.

In practical calculation, since the dynamical mass of a quark is infrared dominant, the scalar part of the inverse quark propagator at zero momentum $B(0,\tilde{\omega}_0^2)$ is a good representation for the chiral property of the quark. We can see it clearly through introducing a cutoff $\Lambda \geq B(0)$ and simply estimating the mass function in the quark propagator with $B(0)$. The integral of the quark propagator in calculating the quark condensate is then proportional to $B(0)\Lambda^2$. Therefore, the chiral susceptibility can be simply rewritten as [28]

$$\chi(0,\tilde{\omega}_0) = \frac{\partial}{\partial m_0}B(0,\tilde{\omega}_0^2). \tag{26}$$

In short, our above analysis indicates that the chiral susceptibility criterion is exactly equivalent to the thermodynamical potential criterion in analyzing a phase transition. Especially, in the case in which one could not have the (effective) thermodynamical potential Γ when completely considering the nonperturbative effect, the chiral susceptibility criterion can still work well. In this paper, we take the two light-flavor quarks, u/d quarks, with degenerate bare mass $m_0 = 3.4$ MeV as our calculated objects to analyze the criteria of the chiral phase transition and verify the equivalence of the different expressions of the chiral susceptibility in practical usage via calculations in the DS equation scheme with the refined quark-gluon interaction vertex. It should also be mentioned that the parameters used in our practical calculations are $\eta = 0.65$ in the refined vertex, the same as in Ref. [102]; $(\mathcal{D}\omega)^{1/3} = 0.52$ GeV and $\omega = 0.5$ GeV in the dressed-gluon propagator, except for looking over specifically the parameter dependence. Because of a lack of knowledge about the interplay between the nonperturbative and perturbative regions, we take the perturbative part [the second term in Eq. (15)] as that preserving the one-loop renormalization-group behavior with $N_F = 4$, which has been shown to be quite reasonable (see, e.g., Refs. [83,97,102,140]). It is known that in a calculation that includes the Yang-Mills sector it is the quark-loop content that controls the number of fermion flavors (see, e.g., Refs. [27,29,32,33,77,104] in DS equation calculations). The Yang-Mills sector in our calculation is only taken into account via a model for the effective interaction, and thus we cannot attentively discuss the flavor of the system. However, as the interaction kernel has been constrained with the hadron properties (see, e.g., Refs. [102,110]), what we do here is to implement a realistic model to represent the real system of QCD, and then from this interaction kernel, we expect the results to be able to explain the experiment data.

B. Numerical results

First, we calculate the quark condensate with Eqs. (23) and (21). The obtained result of the temperature dependence of the condensate at zero chemical potential scaled with that at zero temperature and the comparison with those [more concretely, the light-flavor quark condensate of three-flavor system, $\Delta_{l,s} = \langle\bar{q}q\rangle_l - (m_l/m_s)\langle\bar{q}q\rangle_s$] given in other DS equation calculations [32] and lattice QCD simulation [141] are shown in Fig. 1. The obtained result of the temperature dependence of the scaled condensate at a sizeable quark chemical potential (150 MeV) and the quark

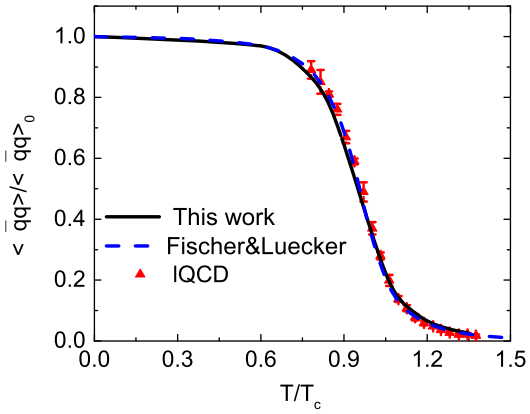

FIG. 1. Calculated scaled quark condensate (solid line) at $\mu = 0$ as a function of $T/T_c(\mu = 0)$ compared with the results (of $\Delta_{l,s}$) from other DS equation calculations (dashed line, taken from Ref. [32]) and lattice QCD simulation (filled triangles with error bars, taken from Ref. [141].)

chemical potential dependence of the scaled condensate at a finite temperature (110 MeV) are shown in Fig. 2.

Looking over Fig. 1, one can easily recognized that our presently calculated temperature dependence of the condensate agrees with the lattice QCD simulation result and the previous DS equation calculation result excellently. In general, the condensate at low temperature barely changes as the temperature increases till about $T \sim 0.8T_c$ with T_c, the inflection points of the corresponding curves (in our calculation, $T_c = 150.8$ MeV). Straightforwardly, T_c is the temperature for the $\frac{\partial\langle\bar{q}q\rangle}{\partial T}$, which is one kind of definition of chiral susceptibility, to reach its maximum. In turn, it is commonly regarded as the (pseudo)critical temperature of the chiral phase transition (specifically, a crossover in the case beyond the chiral limit). In contrast to the continuous evolution at zero chemical potential, Fig. 2 manifests evidently that, in the high chemical potential region, both the temperature and the chemical potential dependences of the quark condensate become discontinuous. In more detail, the condensates for the Nambu solution and Wigner solution are separated in a special region; they "jump to" each other at two distinct chemical potentials, $\mu_{c,l}$ and $\mu_{c,h}$. These features indicate apparently that the phase transition becomes first order, and the region $\mu \in [\mu_{c,l}, \mu_{c,h}]$ and the counterpart of the temperature are just the coexistence regions.

As discussed in Sec. II, besides the $\frac{\partial\langle\bar{q}q\rangle}{\partial T}$, we have other definitions for the chiral susceptibility, such as $\frac{\partial\langle\bar{q}q\rangle}{\partial m_0}$, even the simplified one in practical calculation, $\chi(0,\tilde{\omega}_0) = \frac{\partial B(0,\tilde{\omega}_0^2)}{\partial m_0}$ (e.g., Refs. [27–29]). We should then check the equivalence of the critical temperature and the critical chemical potential determined with the different criteria. In the region of the first- or/and second-order phase transition, due to the functional relation among the dynamical mass, the quark condensate, and the $B(0,\tilde{\omega}_0^2)$, the

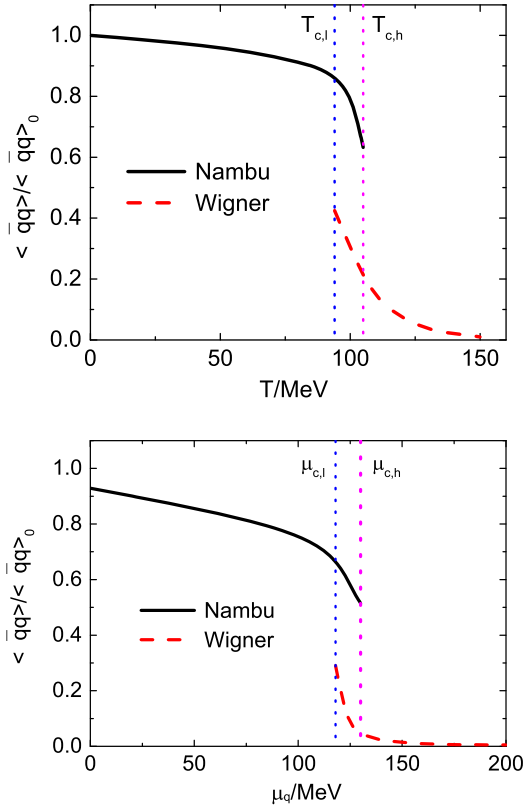

FIG. 2. Calculated scaled quark condensate at $\mu_q = 150$ MeV as a function of T (*upper panel*: *Solid line*–Nambu phase; *dashed line*–Wigner phase) and that at $T = 110$ MeV as a function of μ_q (*lower panel*: *Solid line*–Nambu phase; *dashed line*–Wigner phase).

discontinuities of them are the same (the ones corresponding to the Wigner solution all emerge at the $T_{c,l}$ or/and $\mu_{c,l}$, and those relating to the Nambu solution all disappear at the $T_{c,h}$ or/and $\mu_{c,h}$). All the chiral susceptibilities defined in terms of $B(0,\tilde{\omega}_0^2)$ and $\langle\bar{q}q\rangle$ diverge at the same $T_{c,l}$ ($\mu_{c,l}$) for the Wigner phase, and the same $T_{c,h}$ ($\mu_{c,h}$) for the Nambu phase. Therefore the susceptibility criterion with different definitions of the susceptibility gives definite critical state ($T_{c,l}$, $\mu_{c,l}$) [($T_{c,h}$, $\mu_{c,h}$)] for the first- and second-order phase transitions. While, for the crossover, since the susceptibility does not diverge and there are no rigorous manifestations but just pseudo-critical condition (for both temperature and chemical potential) to mark the DCS restoration, different criteria might give different results. We should thus compare the results fixed with different definitions of the chiral susceptibility carefully. To this end, we give the calculated temperature dependence of chiral susceptibility defined as $\frac{\partial\langle\bar{q}q\rangle}{\partial T}$, $\frac{\partial\langle\bar{q}q\rangle}{\partial m_0}$, and $\frac{\partial B(0,\tilde{\omega}_0^2)}{\partial m_0}$ at zero chemical potential in Fig. 3. The figure manifests evidently that the variation behaviors of the susceptibilities defined differently with respect to the temperature are generally almost the same, which exhibits

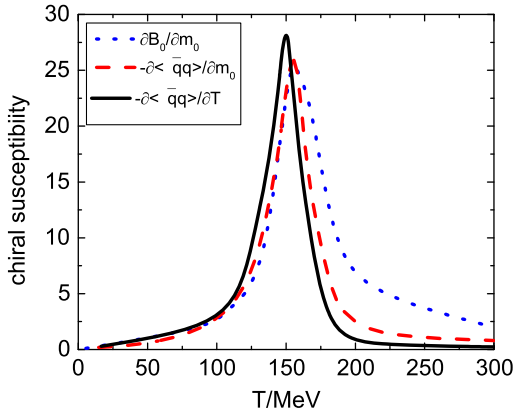

FIG. 3. Calculated $\frac{\partial\langle\bar{q}q\rangle}{\partial T}$, $\frac{\partial\langle\bar{q}q\rangle}{\partial m_0}$, and $\frac{\partial B(0,\tilde{\omega}_0^2)}{\partial m_0}$ at $\mu = 0$ as functions of temperature T (in the *solid line*, *dashed line*, and *dotted line*, respectively).

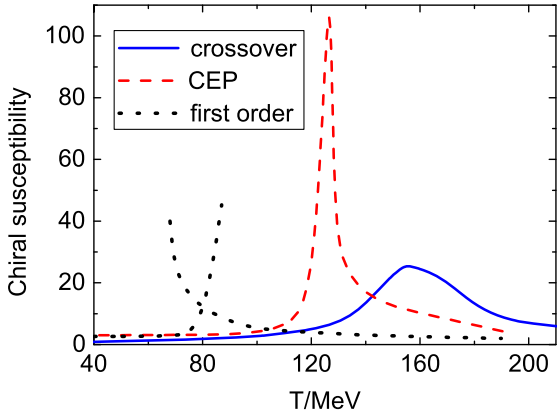

FIG. 4. General characteristics of the chiral susceptibility in different regions (*solid*—at $\mu_q = 0$, i.e., in the crossover region; *dotted*—at $\mu_q = 200$ MeV, i.e., in the first-order transition region; *dashed*—at $\mu_q = 85$ MeV, i.e., near the chemical potential separating the crossover region from the first-order transition region.)

an obvious peak, nevertheless those in terms of the quark condensate show a little sharper than the other one. The continuous variation features of the susceptibilities with different definitions confirm that the chiral phase transition of the system composed of quarks with physical mass is not a sharp phase transition but a crossover. The fact that the two susceptibilities defined as the derivative against the current quark mass have their maxima at the same temperature demonstrates that these two criteria are equivalent to each other, and gives a pseudocritical temperature $T_c(\mu = 0) = 156.1$ MeV. However, the susceptibility defined as the derivative with respect to temperature gives a pseudocritical temperature $T_c(\mu = 0) = 150.8$ MeV, which has been quoted as T_c in last paragraph. These values are definitely highly consistent with the lattice QCD simulation results [13,23,26]. It is well known that the crossover means a smooth evolution from one phase to another, and different criteria lead naturally distinct pseudocritical temperature. The approximately 5 MeV difference (almost the same as that given for three-flavor system in Ref. [32]) among the pseudocritical temperatures determined with different definitions of the chiral susceptibility (i.e., different criteria) is just a manifestation of the crossover. Since the discrepancy among the pseudocritical temperatures obtained with different definitions of the chiral susceptibility is quite small, we will then implement the commonly taken definition of the chiral susceptibility (i.e., that defined as the derivative with respect to the temperature) as the signature to fix the phase diagram in the following.

Figures 1 and 2 manifest apparently that the order parameter, scaled chiral quark condensate, behaves distinctly in the regions of different order phase transitions. In turn, the chiral susceptibility demonstrates different features in the different regions. The calculated temperature dependence of the chiral susceptibilities at three typical values of the chemical potential is shown in Fig. 4. It is apparent that in the first-order transition region, the susceptibility of the Nambu (DCSB) phase diverges at locations different from those for the Wigner (DCS) phase to diverge. The region between the states for the susceptibility of each of the two phases to diverge individually is the coexistence region. In the crossover region, the susceptibility is a smooth function involving a peak, i.e., the susceptibility of the DCSB phase links with (in fact, changes to) that of the DCS phase not only continuously but also smoothly. In the second-order transition region, the susceptibility of the DCSB phase diverges at the same location as that for the susceptibility of the DCS phase to diverge. The characteristic for the susceptibilities of the two phases to diverge at the same location thus defines the state which separates the crossover region from the first-order transition region, namely, the CEP. Therefore, the chiral susceptibility criterion can not only give the phase boundary of the chiral phase transition but also localize the position of the CEP.

IV. DECONFINEMENT PHASE TRANSITION

A. Criterion for deconfinement transition

The confinement is defined as that the color degrees of freedom are confined within hadrons and could not be observed as isolated states. It means that there does not exist an asymptotic free colored state. In turn, it can naturally be represented by the violation of the positivity of the spectral density function. It has been shown that such a violation of the positivity associates the confinement with the dynamically driven changes in the analytical structure of QCD's propagators and vertices [71,142–147]. To avoid the difficulty in calculating the spectral density function, one usually links it with the Schwinger function. The Schwinger function at finite temperature and finite chemical potential is defined as the Fourier transformation of the propagator [55–62],

$$D_{\pm}(\tau,|\vec{p}|=0)=T\sum_{n}e^{-i\omega_n\tau}S_{\pm}(i\omega_n+\mu,|\vec{p}|=0)$$
$$=\int_{-\infty}^{+\infty}\frac{d\omega}{2\pi}\rho_{\pm}(\omega,|\vec{p}|=0)\frac{e^{-(\omega+\mu)\tau}}{1+e^{-(\omega+\mu)/T}}, \quad (27)$$

where $S_{\pm}$ is the projected quark propagator defined as $S=S_{+}L_{+}+S_{-}L_{-}$ with $L_{\pm}=\frac{1}{2}(1\pm\gamma_4)$ and $\rho_{\pm}$ is the corresponding spectral density function and is positive definite if the propagator contains an asymptotic state. The violation of the positivity of the spectral density function is sufficient for determining the confinement [53,54], while the Schwinger function criterion fails in some cases [63]. This is because the Schwinger function is the integral of the spectral density function, even though there exists negativity in the spectral density function, the Schwinger function can still be positive after the integration. The positivity of the Schwinger function is just a prerequisite but not a sufficient condition for judging the deconfinement as found in the calculation in the DS equation approach [63]. It would then be very helpful if one can find a way for the Schwinger function, which is easy to calculate, to represent the properties of spectral density function directly.

Noticing that by differentiating the Schwinger function against the τ we have

$$D_{\pm}^{2n}(\tau,|\vec{p}|)$$
$$=\int_{-\infty}^{+\infty}\frac{d\omega}{2\pi}(\omega+\mu)^{2n}\rho_{\pm}(\omega,|\vec{p}|)\frac{e^{-(\omega+\mu)\tau}}{1+e^{-(\omega+\mu)/T}}, \quad (28)$$

where D^{2n} is the $2n$-order derivative of D. If discretizing the variables in Eq. (28), we have

$$D^{2n}(\tau_l)=\sum_{m}f^{n}(\omega_m,\tau_l)\rho(\omega_m).$$

The $(n\times l)$-dimensional functions $D^{2n}(\tau_l)$ are able to determine the $m=n\times l$-dimensional discretized spectral density function. It can definitely reach to the continuum limit when $n\to\infty$. This means that, even though the Schwinger function D^0 is not sufficient, the series of D^{2n} can determine the properties of the spectral density function completely. If the spectral density function is positive definite, the series of D^{2n} should be all positive, and otherwise, when the spectral density function is somehow negative, negativity will appear in the series of D^{2n} as n reaches a proper (large) value.

B. Numerical result

To show the validity of our criterion, we have calculated the $D(\tau)$, the second-order derivative $D^2(\tau)$, the fourth-order derivative $D^4(\tau)$, and the sixth-order derivative $D^6(\tau)$ at many states (T,μ_q). The obtained results at $(1.1T_c,0)$ and $(0.8T_c,0)$, the spectral density functions of which have been analyzed explicitly in Ref. [61], and those at (140, 110) and (80, 110) MeV are illustrated in Fig. 5.

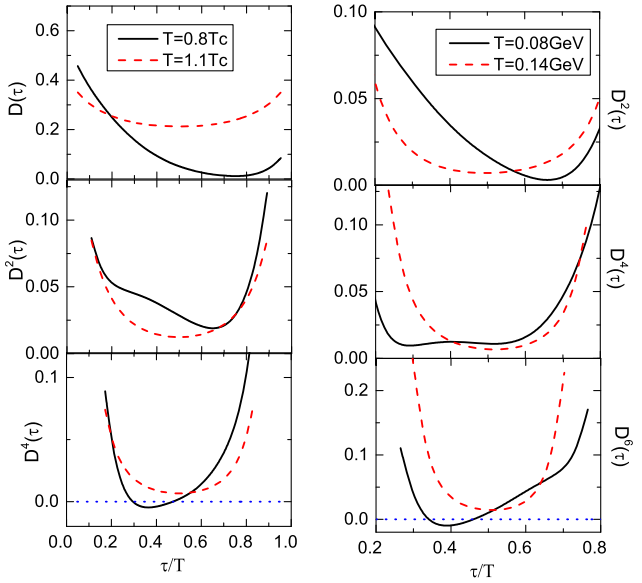

FIG. 5. Calculated Schwinger function $D(\tau)$ and its derivatives $D^2(\tau)$, $D^4(\tau)$ at zero chemical potential (*left panel*: *dashed*—$T=1.1T_c^{\chi}$, *solid*—$T=0.8T_c^{\chi}$) and the $D^2(\tau)$, $D^4(\tau)$, $D^6(\tau)$ at chemical potential $\mu_q=110$ MeV (*right panel*: *dashed*—$T=140$ MeV, *solid*—$T=80$ MeV).

Figure 5 manifests evidently that in the case of zero chemical potential, the $D(\tau)$ at $T=1.1T_c^{\chi}$ is positive definite, which is consistent with the positivity of the spectral density function (see, e.g., Ref. [61]). The $D(\tau)$ at $T=0.8T_c^{\chi}$ is positive definite, too; however, the positivity of the spectral density function is violated (see, e.g., Ref. [61]). Inconsistency emerges in the Schwinger function criterion and the spectral density function criterion. Nevertheless, the $D^4(\tau)$ accords with the spectral density function excellently. In the case of chemical potential $\mu_q=110$ MeV ($\mu_B=330$ MeV), the $D(\tau)$, $D^2(\tau)$ and even $D^4(\tau)$ are all positive, which could not illustrate the confinement nature at $T=80$ MeV, while positivity violation appears for $D^6(\tau)$. It is then clear that analyzing the even-order derivative of the Schwinger function (we refer to it as the generalized Schwinger function hereafter) can play the role of identifying the confinement-deconfinement phase transition efficiently.

From Fig. 5, one can also observe that the positivity violation of the generalized Schwinger function connects the change of the monotonicity of the function. In general, if the $D(\tau)$ and its $2n$-order derivatives are all convex functions, they and the spectral function are positive definite and manifest the deconfinement. While any concave behavior appears in $D^{2n}(\tau)$, positivity violation emerges for the $D^{2(n+1)}(\tau)$ and the spectral density function, which means a confinement.

V. PHASE DIAGRAMS AND CRITICAL END POINT

With the solutions of the quark's DS equation, we can take the chiral susceptibility criterion and the generalized Schwinger function criterion to give the complete phase diagrams in the T–μ plane. For chiral susceptibility, we perform our calculations with definitions $\frac{\partial\langle\bar{q}q\rangle}{\partial T}$, $\frac{\partial\langle\bar{q}q\rangle}{\partial m_0}$, and $\frac{\partial B(0,\tilde{\omega}_0^2)}{\partial m_0}$. The calculated results with each of the definitions show that in the low chemical potential region the line demonstrating the states for the susceptibility of the Nambu phase to take its maximum overlaps with the line for that of the Wigner phase to take its maximum. However, the two lines separate from each other in the high chemical potential region. This indicates that chiral phase transition in the high chemical potential region is a first-order phase transition but that in the low chemical potential region is in fact a crossover, just as mentioned in Sec. III. And there exists a CEP to separate the two regions. The obtained chiral phase diagram with the conventional definition of the chiral susceptibility $\frac{\partial\langle\bar{q}q\rangle}{\partial T}$ and that of the confinement phase diagram are displayed in Fig. 6. It is evident that the presently obtained phase diagram is qualitatively the same as the previous results.

Looking over the numerical data, we notice that our present calculation with the refined quark-gluon interaction vertex (CLR model) gives the position of the CEP at $(\mu_E^B, T_E) = (262.3, 126.3)$ MeV ($\mu_E^B = 3\mu_E^q$), which yields the ratios $T_E/T_c = 0.84$, $\mu_E^B/T_c = 1.74$, and $\mu_E^B/T_E = 2.08$, which agree with the lattice QCD simulation results [15,16,21,25] very well. The ratios are also comparable with the recent DS equation result with the baryon effect being included [77].

Comparing such a result with our previous results in the case beyond chiral limit [34,76], one can observe that both the chemical potentials and the temperatures of the CEP determined via different truncation schemes change accordingly (even though the amplitudes are different). To investigate the parameter dependence of the location of the CEP, we have performed a series of calculations, maintaining the same quark condensate at $T = \mu = 0$. Our calculated results indicate that, to keep the quark condensate the same, the parameter ω in the interaction can take different values but the $\mathcal{D}$ should be almost a constant. Moreover, as the parameter ω decreases, the μ_E decreases, and the T_E increases. Some of the concrete data are listed in Table I. Extending the idea discussed in Refs. [28,48,76], one can infer that the $\frac{1}{\omega}$ plays the role of the radius of the interaction sphere. An increase of the interaction radius (i.e., the volume of the interaction sphere) plays the same role as increasing the density of the system; it compensates then the effect of increasing the chemical potential. As a consequence, the μ_E^B decreases, and the T_E increases simultaneously due to the compensation.

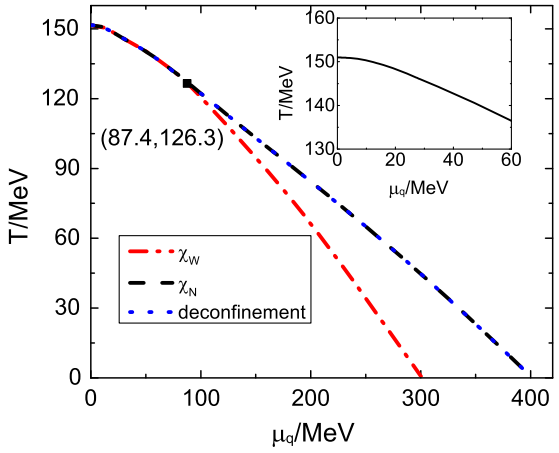

FIG. 6. Calculated phase diagrams on the T–μ_q plane (*dotted-dashed*—Wigner chiral phase transition; *dashed*—Nambu chiral phase transition; *dotted*—Deconfinement phase transition.)

If we consider only the crossover region of the chiral phase transition, we can fit the chiral phase boundary line with an expansion formula,

$$T_c(z = \mu/T_{c,\mu}) = T_{c,\mu=0}(1 - \kappa z^2), \tag{29}$$

with $\kappa = 0.339$ if μ stands for that of the quarks and $\kappa_B = 0.038$ if μ refers to the baryon chemical potential. This value is merely one time larger than that given in recent lattice QCD simulations [typically around 0.018] [19,20,24], and consistent with other DSEs calculations [29,33,34,76,77]. Since lattice QCD simulation suffers from the sign problem at finite chemical potential and thus usually employs the techniques like Taylor expansion or analytic continuation, we believe it would be reliable to determine the curvature parameter through the DS equation approach, which does not involve further approximation when carrying out the calculation on the finite chemical potential domain.

For the first-order phase transition region, people usually take the phase equilibrium condition $P_N = P_W$ to fix the boundary line. Even though we could not give the boundary line in such a way now since we could not get the thermodynamical potential due to including the nonperturbative effect more generally in the presently

TABLE I. Calculated parameter dependence of the location of the CEP (μ_E^B, T_E) via different truncation schemes with the quark condensate $\langle\bar{q}q\rangle_{\mu=1\,\mathrm{GeV}}$ being kept a constant [$(240\ \mathrm{MeV})^3$] (all the dimensional quantities are in the unit GeV).

Scheme	$(D\omega)^{1/3}$	ω	T_c	(μ_E^B, T_E)	μ_E^B/T_E
Bare	0.800	0.450	0.1562	(0.2055,0.1524)	1.3572
	0.800	0.500	0.1503	(0.3324,0.1283)	2.5908
	0.800	0.550	0.1343	(0.4371,0.1143)	3.8241
Refined	0.501	0.450	0.1536	(0.1176,0.1513)	0.7773
	0.520	0.500	0.1508	(0.2623,0.1263)	2.0768
	0.536	0.550	0.1274	(0.3909,0.1022)	3.8247

refined truncation scheme, one can infer that the line must be located between the (red) dotted-dashed line and the (black) dashed line. From the condition $P_N = P_W$, we directly have

$$\frac{d(P_N - P_W)}{dT} = \left(\frac{\partial P_N}{\partial \mu} - \frac{\partial P_W}{\partial \mu}\right)\frac{\partial \mu}{\partial T} + \left(\frac{\partial P_N}{\partial T} - \frac{\partial P_W}{\partial T}\right) = 0.$$

With the thermodynamical relations $n = \partial P/\partial \mu$ and $s = \partial P/\partial T$, where n is the particle number density and s is the entropy density, we observe

$$\frac{\partial \mu}{\partial T} = -\frac{s_N - s_W}{n_N - n_W}. \tag{30}$$

Typically, the DCS phase has a larger entropy density and a larger quark number density, which reads $n_W > n_N$ and $s_W > s_N$. Therefore, one should have $\frac{\partial \mu}{\partial T} < 0$. It indicates that the phase boundary line $T(\mu_q)$ will always decrease monotonically as the μ_q increases and could not involve any backbend. Such a feature can be extended to the crossover region since where the pressure equilibrium condition is still satisfied. In more specific case, $\mu = 0$ (or $\mu \to 0^+$), due to the conjugate symmetry of the $\pm\mu$, we have $\frac{\partial T}{\partial \mu} = 0$. As a consequence, the boundary curve hits the vertical (T) axis perpendicularly. Figure 6, especially the insertion, manifests evidently that our numerical result coincides with the general principle excellently, and so do the previous DS equation calculation results (e.g., Refs. [27–34,76–78]), lattice QCD simulation results, and other model results (e.g., Ref. [46]).

Furthermore, for the confinement-deconfinement phase transition, our presently calculated result, as shown in Fig. 6, manifests that the dotted curve determined with $D^4(\tau) = 0$ or $D^6(\tau) = 0$ overlaps with the chiral phase transition line of the Nambu phase. It indicates that the deconfinement phase transition coincides with the complete chiral symmetry restoration (chiral phase transition) exactly, and it makes the locations of the two kinds of CEPs coincide. Meanwhile, the Wigner phase is always in the deconfinement phase even when it is unstable in the low temperature and low chemical potential region. This feature provides evidence again that hierarchy between the chiral phase transition and the deconfinement phase transition does not exist.

In addition, if we employ the parametrization of the chemical freeze-out condition reported in Ref. [113], we would propose that the CEP may appear in the matter generated by the Au-Au collision at the energy $\sqrt{s} \cong$ 14.6 GeV, or with the parametrization in Ref. [114], we obtain $\sqrt{s} \cong 13.9$ GeV. If we take further the finite size effect into account [78], the energy to generate the CEP in the Au-Au collision will shift to $\sqrt{s} \cong 9.4$ GeV. By fitting the data from lattice QCD simulation [115] with the energy dependence expression $\mu_B = d/(1 + e\sqrt{s})$, we can also find that the CEP can be reached in the matter generated by the Au-Au collision with center-of-mass energy $\sqrt{s} \cong 10$ GeV. Such an energy range 9–15 GeV is consistent with what the oscillation structure of the net baryon number fluctuation observed in recent RHIC experiments [117] hints.

VI. SUMMARY

With the refined truncation scheme of the Dyson-Schwinger equations developed recently, with which the dressed quark-gluon interaction vertex is written in a quite concise form, we studied the QCD phase transitions in this paper. For the chiral phase transition, we analyzed the equivalence of the (generalized) chiral susceptibility criterion and the thermodynamical potential criterion. The chiral susceptibility criterion is much more powerful in the case of taking the nonperturbative nature of the phase transitions into account where the thermodynamical potential is not available. We also investigated the consistency of the chiral susceptibility criterion with distinct definitions of the susceptibility (i.e., that in different directions) and showed that the susceptibility along different directions behaves in the same manner in the first-order transition region but slightly differently in the crossover region. For the deconfinement phase transition, we gave a generalized Schwinger function criterion and proved that the positivity violation of the generalized Schwinger function is definitely a sufficient condition to identify the confinement.

With these criteria and the solutions of the refined DS equations, we obtained the complete phase diagram of not only the chiral phase transition but also the deconfinement transition. The results indicate that the two kinds of phase transitions coincide with each other completely. Our results for the chiral phase transition predict that there exists a CEP and it is located at $(\mu_E^B, T_E) = (262.3, 126.3)$ MeV, with $T_E/T_c = 0.84$ and $\mu_E^B/T_c = 1.74$, which agrees with lattice QCD simulation results and former DS equation results very well. The obtained phase boundary coincides with the lattice QCD simulation and previous DS equation calculation results well, and matches the requirement of the general principle in Eq. (30). With the parametrization for the collision energy dependence of the chemical potential, we propose that the CEP may appear in the states generated by the $\sqrt{s} \cong$ 9–15 GeV Au-Au collision.

Comparing our presently obtained results with the refined truncation scheme and the (previous) ones with the bare vertex approximation, one can notice that an obvious discrepancy between the results via different truncation schemes in general does not exist. However, the refined scheme shifts the location of the CEP to lower chemical potential and higher temperature. It provides evidence for that the CEP locates in the region of the states that the presently planned RHIC experiments could generate. Nevertheless, since present experiments can not provide information for the states above the chemical freeze-out line but the CEP is a specific state at the phase

boundary, plenty of works are then required in order to detect the CEP in experiments. Exploring the chemical freeze-out conditions with the refined truncation scheme is thus in progress. In addition, the work to distinguish the longitudinal part from the transverse part of the dressed-gluon propagator is also in progress.

ACKNOWLEDGMENTS

The work was supported by the National Natural Science Foundation of China under Contract No. 11435001 and the National Key Basic Research Program of China under Contracts No. G2013CB834400 and No. 2015CB856900.

[1] P. Braun-Munzinger and J. Wambach, Rev. Mod. Phys. **81**, 1031 (2009).
[2] K. Fukushima and T. Hatsuda, Rep. Prog. Phys. **74**, 014001 (2011).
[3] O. Philipsen, Prog. Part. Nucl. Phys. **70**, 55 (2013).
[4] R. D. Pisarski and F. Wilczek, Phys. Rev. D **29**, 338 (1984).
[5] F. Karsch and E. Laermann, Phys. Rev. D **50**, 6954 (1994).
[6] T. Hatsuda and T. Kunihiro, Phys. Rep. **247**, 221 (1994).
[7] Z. Fodor and S. D. Katz, Phys. Lett. B **534**, 87 (2002).
[8] P. de Forcrand and O. Philipsen, Nucl. Phys. **B642**, 290 (2002); **B673**, 170 (2003); Ph. de Forcrand and S. Kratochvila, Nucl. Phys. B, Proc. Suppl. **153**, 62 (2006).
[9] Z. Fodor and S. D. Katz, J. High Energy Phys. 03 (2002) 014; Z. Fodor and S. D. Katz, J. High Energy Phys. 04 (2004) 050.
[10] M. D'Elia and M. P. Lombardo, Phys. Rev. D **67**, 014505 (2003).
[11] C. Bernard, T. Burch, C. DeTar, J. Osborn, S. Gottlieb, E. B. Gregory, D. Toussaint, U. M. Heller, and R. Sugar, Phys. Rev. D **71**, 034504 (2005).
[12] Y. Aoki, G. Endrodi, Z. Fodor, S. D. Katz, and K. K. Szabo, Nature (London) **443**, 675 (2006).
[13] Y. Aoki, Z. Fodor, S. D. Katz, and K. K. Szabo, Phys. Lett. B **643**, 46 (2006).
[14] C. R. Allton, M. Doring, S. Ejiri, S. J. Hands, O. Kaczmarek, F. Karsch, E. Laermann, and K. Redlich, Phys. Rev. D **71**, 054508 (2005).
[15] R. V. Gavai and S. Gupta, Phys. Rev. D **71**, 114014 (2005); **78**, 114503 (2008).
[16] C. Schmidt (RBC-Bielefeld Collaboration), J. Phys. G **35**, 104093 (2008).
[17] Z. Fodor and S. D. Katz, arXiv:0908.3341.
[18] Ph. de Forcrand and O. Philipsen, Phys. Rev. Lett. **105**, 152001 (2010); Ph. de Forcrand, J. Langelage, O. Philipsen, and W. Unger, Phys. Rev. Lett. **113**, 152002 (2014).
[19] G. Endrodi, Z. Fodor, S. D. Katz, and K. K. Szabo, J. High Energy Phys. 04 (2011) 001.
[20] O. Kaczmarek, F. Karsch, E. Laermann, C. Miao, S. Mukherjee, P. Petreczky, C. Schmidt, W. Soeldner, and W. Unger, Phys. Rev. D **83**, 014504 (2011).
[21] A. Li, A. Alexandru, and K. F. Liu, Phys. Rev. D **84**, 071503 (2011).
[22] F. Karsch, B. J. Schaefer, M. Wagner, and J. Wambach, Phys. Lett. B **698**, 256 (2011).
[23] A. Bazavov *et al.*, Phys. Rev. D **85**, 054503 (2012).
[24] P. Cea, L. Cosmai, and A. Papa, Phys. Rev. D **89**, 074512 (2014).
[25] S. Gupta, N. Karthik, and P. Majumdar, Phys. Rev. D **90**, 034001 (2014).
[26] T. Bhattacharya *et al.*, Phys. Rev. Lett. **113**, 082001 (2014).
[27] C. S. Fischer and J. A. Mueller, Phys. Rev. D **80**, 074029 (2009); C. S. Fischer, J. Luecker, and J. A. Mueller, Phys. Lett. B **702**, 438 (2011).
[28] S. X. Qin, L. Chang, H. Chen, Y. X. Liu, and C. D. Roberts, Phys. Rev. Lett. **106**, 172301 (2011).
[29] C. S. Fischer and J. Luecker, Phys. Lett. B **718**, 1036 (2013).
[30] M. He, Y. Jiang, W. M. Sun, and H. S. Zong, Phys. Rev. D **77**, 076008 (2008); M. He, F. Hu, W. M. Sun, and H. S. Zong, Phys. Lett. B **675**, 32 (2009); B. Wang, Z. F. Cui, W. M. Sun, and H. S. Zong, Few-Body Syst. **55**, 47 (2014); C. Shi, Y. L. Wang, Y. Jiang, Z. F. Cui, and H. S. Zong, J. High Energy Phys. 07 (2014) 014; S. S. Xu, Z. F. Cui, B. Wang, Y. M. Shi, Y. C. Yang, and H. S. Zong, Phys. Rev. D **91**, 056003 (2015); Y. Lu, Z. F. Cui, Z. Pan, C. H. Chang, and H. S. Zong, Phys. Rev. D **93**, 074037 (2016).
[31] E. Gutiérrez, A. Ahmad, A. Ayala, A. Bashir, and A. Raya, J. Phys. G **41**, 075002 (2014).
[32] C. S. Fischer, J. Luecker, and C. A. Welzbacher, Phys. Rev. D **90**, 034022 (2014).
[33] C. S. Fischer, J. Luecker, and C. A. Welzbacher, Nucl. Phys. **A931**, 774 (2014).
[34] F. Gao, J. Chen, Y. X. Liu, S. X. Qin, C. D. Roberts, and S. M. Schmidt, Phys. Rev. D **93**, 094019 (2016).
[35] Y. Hatta and M. A. Stephanov, Phys. Rev. Lett. **91**, 102003 (2003).
[36] S. K. Ghosh, T. K. Mukherjee, M. G. Mustafa, and R. Ray, Phys. Rev. D **73**, 114007 (2006).
[37] B. J. Schaefer, J. M. Pawlowski, and J. Wambach, Phys. Rev. D **76**, 074023 (2007).
[38] B. J. Schaefer and M. Wagner, Phys. Rev. D **79**, 014018 (2009).
[39] C. Sasaki, B. Friman, and K. Redlich, Phys. Rev. D **75**, 074013 (2007).
[40] W. J. Fu, Z. Zhang, and Y. X. Liu, Phys. Rev. D **77**, 014006 (2008).
[41] M. Ciminale, R. Gatto, N. D. Ippolito, G. Nardulli, and M. Ruggieri, Phys. Rev. D **77**, 054023 (2008).
[42] C. Sasaki, B. Friman, and K. Redlich, Phys. Rev. D **77**, 034024 (2008).

[43] P. Costa, M. C. Ruivo, and C. A. de Sousa, Phys. Rev. D **77**, 096001 (2008).
[44] K. Fukushima, Phys. Rev. D **77**, 114028 (2008).
[45] H. Abuki, R. Anglani, R. Gatto, G. Nardulli, and M. Ruggieri, Phys. Rev. D **78**, 034034 (2008).
[46] A. Ayala, A. Bashir, C. A. Dominguez, E. Gutiérrez, M. Loewe, and A. Raya, Phys. Rev. D **84**, 056004 (2011).
[47] T. Sasaki, Y. Sakai, H. Kouno, and M. Yahiro, Phys. Rev. D **82**, 116004 (2010); L. J. Jiang, X. Y. Xin, K. L. Wang, S. X. Qin, and Y. X. Liu, Phys. Rev. D **88**, 016008 (2013).
[48] X. Y. Xin, S. X. Qin, and Y. X. Liu, Phys. Rev. D **89**, 094012 (2014).
[49] B. Mohanty, Nucl. Phys. **A830**, 899 (2009).
[50] R. A. Lacey, Phys. Rev. Lett. **114**, 142301 (2015).
[51] R. A. Lacey, A. Taranenko, J. Jia, D. Reynolds, N. N. Ajitanand, J. M. Alexander, Yi Gu, and A. Mwai, Phys. Rev. Lett. **112**, 082302 (2014).
[52] Y. Zhao, L. Chang, W. Yuan, and Y. X. Liu, Eur. Phys. J. C **56**, 483 (2008).
[53] C. D. Roberts and A. G. Williams, Prog. Part. Nucl. Phys. **33**, 477 (1994).
[54] R. Alkofer and L. V. Smekal, Phys. Rep. **353**, 281 (2001).
[55] A. Bender, D. Blaschke, Y. Kalinovsky, and C. D. Roberts, Phys. Rev. Lett. **77**, 3724 (1996).
[56] A. Bender, G. I. Poulis, C. D. Roberts, S. M. Schmidt, and A. W. Thomas, Phys. Lett. B **431**, 263 (1998).
[57] A. Bashir, A. Raya, I. C. Cloët, and C. D. Roberts, Phys. Rev. C **78**, 055201 (2008).
[58] A. Bashir, A. Raya, S. Sanchez-Madrigal, and C. D. Roberts, Few-Body Syst. **46**, 229 (2009).
[59] J. A. Mueller, C. S. Fischer, and D. Nickel, Eur. Phys. J. C **70**, 1037 (2010).
[60] S. X. Qin, L. Chang, Y. X. Liu, and C. D. Roberts, Phys. Rev. D **84**, 014017 (2011).
[61] S. X. Qin and D. H. Rischke, Phys. Rev. D **88**, 056007 (2013).
[62] F. Gao, S. X. Qin, Y. X. Liu, C. D. Roberts, and S. M. Schmidt, Phys. Rev. D **89**, 076009 (2014).
[63] R. Alkofer, W. Detmold, C. S. Fischer, and P. Maris, Phys. Rev. D **70**, 014014 (2004).
[64] C. D. Roberts and S. M. Schmidt, Prog. Part. Nucl. Phys. **45**, S1 (2000).
[65] P. Maris and C. D. Roberts, Int. J. Mod. Phys. E **12**, 297 (2003).
[66] C. S. Fischer, J. Phys. G **32**, R253 (2006).
[67] A. Bashir, L. Chang, I. C. Cloet, B. El-Bennich, Y. X. Liu, C. D. Roberts, and P. C. Tandy, Commun. Theor. Phys. **58**, 79 (2012).
[68] I. C. Cloet and C. D. Roberts, Prog. Part. Nucl. Phys. **77**, 1 (2014).
[69] J. M. Pawlowski, Ann. Phys. (Amsterdam) **322**, 2831 (2007).
[70] L. McLerran and R. D. Pisarski, Nucl. Phys. **A796**, 83 (2007).
[71] L. Fister and J. M. Pawlowski, Phys. Rev. D **88**, 045010 (2013).
[72] D. Blaschke, C. D. Roberts, and S. Schmidt, Phys. Lett. B **425**, 232 (1998).
[73] P. Maris, A. Raya, C. D. Roberts, and S. M. Schmidt, Eur. Phys. J. A **18**, 231 (2003).
[74] H. Chen, W. Yuan, L. Chang, Y. X. Liu, T. Klahn, and C. D. Roberts, Phys. Rev. D **78**, 116015 (2008).
[75] C. S. Fischer, Phys. Rev. Lett. **103**, 052003 (2009).
[76] X. Y. Xin, S. X. Qin, and Y. X. Liu, Phys. Rev. D **90**, 076006 (2014).
[77] G. Eichmann, C. S. Fischer, and C. A. Welzbacher, Phys. Rev. D **93**, 034013 (2016).
[78] J. Chen, F. Gao, and Y. X. Liu, arXiv:1510.07543.
[79] M. Mitter, J. M. Pawlowski, and N. Strodthoff, Phys. Rev. D **91**, 054035 (2015).
[80] N. Mueller and J. M. Pawlowski, Phys. Rev. D **91**, 116010 (2015).
[81] N. Christiansen, M. Haas, J. M. Pawlowski, and N. Strodthoff, Phys. Rev. Lett. **115**, 112002 (2015).
[82] W. J. Fu and J. M. Pawlowski, Phys. Rev. D **92**, 116006 (2015); **93**, 091501(R) (2016).
[83] P. Maris and C. D. Roberts, Phys. Rev. C **56**, 3369 (1997); P. Maris and P. C. Tandy, Phys. Rev. C **60**, 055214 (1999).
[84] J. C. Ward, Phys. Rev. **78**, 182 (1950).
[85] H. S. Green, Proc. Phys. Soc. London Sect. A **66**, 873 (1953).
[86] Y. Takahashi, Nuovo Cimento **6**, 371 (1957).
[87] M. Blank and A. Krassnigg, Phys. Rev. D **84**, 096014 (2011); T. Hilger, C. Popovici, M. Gomez-Rocha, and A. Krassnigg, Phys. Rev. D **91**, 034013 (2015).
[88] C. D. Roberts, *Como 1996, Quark Confinement and the Hadron Spectrum II*, edited by N. Brambilla and G. M. Prosperi (World Scientific, Singapore, 1996), p. 224.
[89] C. D. Roberts, Phys. Part. Nucl. **30**, 223 (1999).
[90] A. Bender, W. Detmold, A. W. Thomas, and C. D. Roberts, Phys. Rev. C **65**, 065203 (2002).
[91] M. S. Bhagwat, A. Höll, A. Krassnigg, C. D. Roberts, and P. C. Tandy, Phys. Rev. C **70**, 035205 (2004).
[92] C. J. Burden, L. Qian, C. D. Roberts, P. C. Tandy, and M. J. Thomson, Phys. Rev. C **55**, 2649 (1997).
[93] P. Watson, W. Cassing, and P. C. Tandy, Few-Body Syst. **35**, 129 (2004).
[94] C. S. Fischer and R. Williams, Phys. Rev. Lett. **103**, 122001 (2009).
[95] A. Krassnigg, Phys. Rev. D **80**, 114010 (2009).
[96] T. Hilger, M. Gomez-Rocha, and A. Krassnigg, Phys. Rev. D **91**, 114004 (2015); T. Hilger and A. Krassnigg, arXiv:1605.03464.
[97] S. X. Qin, L. Chang, Y. X. Liu, C. D. Roberts, and D. J. Wilson, Phys. Rev. C **84**, 042202(R) (2011).
[98] S. X. Qin, L. Chang, Y. X. Liu, C. D. Roberts, and D. J. Wilson, Phys. Rev. C **85**, 035202 (2012).
[99] A. Höll, A. Krassnigg, and C. D. Roberts, Phys. Rev. C **70**, 042203(R) (2004); A. Höll, A. Krassnigg, P. Maris, C. D. Roberts, and S. V. Wright, Phys. Rev. C **71**, 065204 (2005).
[100] A. Höll, A. Krassnigg, C. D. Roberts, and S. V. Wright, Int. J. Mod. Phys. A **20**, 1778 (2005).
[101] A. Krassnigg and M. Blank, Phys. Rev. D **83**, 096006 (2011).
[102] L. Chang and C. D. Roberts, Phys. Rev. C **85**, 052201(R) (2012).
[103] M. Gomez-Rocha, T. Hilger, and A. Krassnigg, Few-Body Syst. **56**, 475 (2015); Phys. Rev. D **92**, 054030 (2015); **93**, 074010 (2016).

[104] R. Williams, C. S. Fischer, and W. Heupel, Phys. Rev. D **93**, 034026 (2016).
[105] H. F. Fu and Q. Wang, Phys. Rev. D **93**, 014013 (2016).
[106] A. Ayala and A. Bashir, Phys. Rev. D **64**, 025015 (2001).
[107] A. Kizilersü and M. R. Pennington, Phys. Rev. D **79**, 125020 (2009).
[108] A. Bashir, A. Raya, and S. Sánchez-Madrigal, Phys. Rev. D **84**, 036013 (2011); A. Bashir, R. Bermudez, L. Chang, and C. D. Roberts, Phys. Rev. C **85**, 045205 (2012).
[109] L. Chang, Y. X. Liu, and C. D. Roberts, Phys. Rev. Lett. **106**, 072001 (2011).
[110] D. Binosi, L. Chang, J. Papavassiliou, and C. D. Roberts, Phys. Lett. B **742**, 183 (2015).
[111] H. X. He, Phys. Rev. D **80**, 016004 (2009).
[112] S. X. Qin, L. Chang, Y. X. Liu, C. D. Roberts, and S. M. Schmidt, Phys. Lett. B **722**, 384 (2013); S. X. Qin, C. D. Roberts, and S. M. Schmidt, Phys. Lett. B **733**, 202 (2014).
[113] J. Cleymans, H. Oeschler, K. Redlich, and S. Wheaton, Phys. Rev. C **73**, 034905 (2006).
[114] A. Andronic, P. Braun-Munzinger, and J. Stachel, Nucl. Phys. **A772**, 167 (2006).
[115] S. Borsanyi, Z. Fodor, S. D. Katz, S. Krieg, C. Ratti, and K. K. Szabo, Phys. Rev. Lett. **113**, 052301 (2014).
[116] L. Adamczyk *et al.* (STAR Collaboration), Phys. Rev. Lett. **113**, 092301 (2014).
[117] X. Luo (STAR Collaboration), *Proc. Sci.*, CPOD2014 (2015) 019; X. Luo, Nucl. Phys. **A956**, 75 (2016).
[118] J. S. Ball and T. W. Chiu, Phys. Rev. D **22**, 2542 (1980); Phys. Rev. D **22**, 2550 (1980).
[119] P. Maris, C. D. Roberts, S. M. Schmidt, and P. C. Tandy, Phys. Rev. C **63**, 025202 (2001).
[120] M. H. Thoma, Nucl. Phys. **A638**, 317C (1998).
[121] N. Haque, M. G. Mustafa, and M. Strickland, Phys. Rev. D **87**, 105007 (2013).
[122] A. Cucchieri, A. Maas, and T. Mendes, Phys. Rev. D **75**, 076003 (2007).
[123] C. S. Fischer, A Maas, and J. A. Mueller, Eur. Phys. J. direct C **68**, 165 (2010).
[124] P. J. Silva, O. Oliveira, P. Bicudo, and N. Cardoso, Phys. Rev. D **89**, 074503 (2014).
[125] P. O. Bowman, U. M. Heller, D. B. Leinweber, M. B. Parappilly, and A. G. Williams, Phys. Rev. D **70**, 034509 (2004); P. O. Bowman, U. M. Heller, D. B. Leinweber, M. B. Parappilly, A. G. Williams, and J. B. Zhang, Phys. Rev. D **71**, 054507 (2005).
[126] I. Bogolubsky, E. Ilgenfritz, M. Muller-Preussker, and A. Sternbeck, Phys. Lett. B **676**, 69 (2009).
[127] P. Boucaud, M. E. Gomez, J. P. Leroy, A. Le Yaouanc, J. Micheli, O. Pene, and J. Rodriguez-Quintero, Phys. Rev. D **82**, 054007 (2010).
[128] O. Oliveira and P. Bicudo, J. Phys. G **38**, 045003 (2011).
[129] A. Cucchieri, D. Dudal, T. Mendes, and N. Vandersickel, Phys. Rev. D **85**, 094513 (2012).
[130] A. C. Aguilar, D. Binosi, and J. Papavassiliou, Phys. Rev. D **86**, 014032 (2012).
[131] A. Ayala, A. Bashir, D. Binosi, M. Cristoforetti, and J. Rodriguez-Quintero, Phys. Rev. D **86**, 074512 (2012).
[132] D. Dudal, O. Oliveira, and J. Rodriguez-Quintero, Phys. Rev. D **86**, 105005 (2012).
[133] S. Strauss, C. S. Fischer, and C. Kellermann, Phys. Rev. Lett. **109**, 252001 (2012).
[134] D. Zwanziger, Phys. Rev. D **87**, 085039 (2013).
[135] B. Blossier, Ph. Boucaud, M. Brinet, F. De Soto, V. Morenas, O. Pene, K. Petrov, and J. Rodriguez-Quintero, Phys. Rev. D **87**, 074033 (2013).
[136] J. M. Cornwall, R. Jackiw, and E. Tomboulis, Phys. Rev. D **10**, 2428 (1974).
[137] W. Yuan, H. Chen, and Y. X. Liu, Phys. Lett. B **637**, 69 (2006).
[138] Z. F. Cui, F. Y. Hou, Y. M. Shi, Y. L. Wang, and H. S. Zong, Ann. Phys. (Amsterdam) **358**, 172 (2015).
[139] C. McNeile, A. Bazavov, C. T. H. Davies, R. J. Dowdall, K. Hornbostel, G. P. Lepage, and H. D. Trottier, Phys. Rev. D **87**, 034503 (2013).
[140] G. Eichmann, I. C. Cloët, R. Alkofer, A. Krassnigg, and C. D. Roberts, Phys. Rev. C **79**, 012202(R) (2009).
[141] S. Borsanyi, Z. Fodor, C. Hoelbling, S. D. Katz, S. Krieg, C. Ratti, and K. K. Szabo, J. High Energy Phys. 09 (2010) 073.
[142] V. N. Gribov, Eur. Phys. J. C **10**, 91 (1999).
[143] H. J. Munczek and A. M. Nemirovsky, Phys. Rev. D **28**, 181 (1983).
[144] M. Stingl, Phys. Rev. D **29**, 2105 (1984).
[145] R. T. Cahill, Aust. J. Phys. **42**, 171 (1989).
[146] C. D. Roberts, A. G. Williams, and G. Krein, Int. J. Mod. Phys. A **07**, 5607 (1992).
[147] F. T. Hawes, C. D. Roberts, and A. G. Williams, Phys. Rev. D **49**, 4683 (1994).